OAK RIDGE
NATIONAL LABORATORY
MANAGED BY UT-BATTELLE
FOR THE DEPARTMENT OF ENERGY

ORNL/TM-2011/393

Annex VIII – Thermoelectric Materials for Waste Heat Recovery: An International Collaboration for Transportation Applications

November 30, 2011

Prepared by
Hsin Wang,
Senior Research Staff

UT-BATTELLE
ORNL-27 (4-00)

ORNL/TM-2011/434

Materials Science and Technology

ANNEX VIII – THERMOELECTRIC MATERIALS FOR WASTE HEAT RECOVERY: AN INTERNATIONAL COLLABORATION FOR TRANSPORTATION APPLICATIONS

Hsin Wang[1], Wallace Porter[1], Harold Bottner[2], Jan Konig[2], Lidong Chen[3], Shengqiang Bai[3], Terry Tritt[4], Alex Mayolett[5], Jayantha Senawiratne[5], Charlene Smith[5], Fred Harris[6], Jeff Sharp[7], Jason Lo[8], Holger Kleinke[9], Laszlo Kiss[10]

[1]Oak Ridge National Laboratory, USA
[2]Fraunhofer Institute for Physical Measurement Techniques, Germany
[3]Shanghai Institute of Ceramics, Chinese Academy of Sciences, China
[4]Clemson University, USA
[5]Corning Inc., USA
[6]ZT-Plus Inc. USA
[7]Marlow Industries, USA
[8]CANMET, Canada
[9]University of Waterloo, Canada
[10]University of Quebec at Chicoutimi, Quebec, Canada

Date Published: November 2011

Prepared by
OAK RIDGE NATIONAL LABORATORY
Oak Ridge, Tennessee 37831-6283
managed by
UT-BATTELLE, LLC
for the
U.S. DEPARTMENT OF ENERGY
under contract DE-AC05-00OR22725

CONTENTS

Page

LIST OF FIGURES

TOPICAL REPORT: INTERNATIONAL ROUND-ROBIN TESTING OF BULK TEHRMOELECTRICS

1. Introduction

For almost 60 years between the 1940s and the early 1990s, the highest figure of merit, *ZT*, values of all thermoelectric materials remained close to 1[1-3]. The most reliable TE material continued to be bismuth telluride [4]. Commercial applications of bismuth telluride are cooling devices based on the Peltier effect [1]. The other two state-of-the-art thermoelectrics at high temperatures are PbTe and SiGe [5]. Thermoelectrics found applications in the NASA Apollo lunar missions and in deep space missions including the Viking Mars landers; Pioneer 10 and 11; and the Voyager, Ulysses, Galileo, and Cassini outer-planet spacecraft [6] as power generators. In the meantime, thermoelectrics have also been used in defense related device cooling. In the US, substantial federal funding from Department of Defense (DOD), NASA and Office of Naval Research (ONR) since the early 1990s as well as private enterprise research and development efforts led to significant increases in *ZT* which reinvigorated interests in TE technology. Besides improvement in ZT of the Bi_2Te_3, PbTe and SiGe, new classes of materials have been developed. In the meantime, thermoelectric devices were brought into broader cooling and refrigeration markets by lowering the raw material and manufacturing costs.

The research and development of thermoelectric materials have made significant direct impact on the automotive industry by enhancing air conditioning efficiency and integrated cabin climate control. An excellent example was the use of thermoelectrics in the climate/comfort control of seats in automobiles. The recent high temperature materials development has also shown great potential for converting exhaust heat directly into electricity without additional engine load. For the automotive industry, TE technology could lead to an all-solid-state, reversible (for both heating and cooling) air-conditioning system that does not use refrigerants with greenhouse gas concerns. TE devices may also be used to control the temperature of the battery or other devices in order to increase reliability of batteries and selected energy storage components. The above applications have made thermoelectric devices perfect candidates to be integrated into the plug-in hybrid vehicles and electric vehicles as well as conventional internal combustion engine vehicles.

Since 2005, thermoelectric power generation using automobile waste heat is being realized through the US Department of Energy (DOE) waste heat recovery program and other efforts from the Office of Vehicle Technologies (VT). Another on-going DOE program is focusing on heating and cooling applications of the thermoelectric materials. The remaining challenges in thermoelectric power generation and refrigeration are materials related. First of all, the figure-of-merit, ZT, still needs to improve from the current value of 1.5 to above 2 to be competitive. The transportation applications also put restrictions on the cost. In the meantime, the thermoelectric community could greatly benefit from the development of international test standards, improved test methods and better characterization tools.

Internationally, thermoelectrics have been recognized by many countries as an important area for energy efficiency. In North America, USA and Canada are the two major countries for the advancement of thermoelectrics. In Asia, countries like Japan, China and South Korea have been

very active in the development of thermoelectric materials and devices. Europe was the birthplace of thermoelectrics and it has a long tradition for materials development and applications. Countries such as United Kingdom, Germany, France, Russia, and Austria have been the hosts of multiple European and international thermoelectric conferences. Most of these countries are already members of the International Energy Agency (IEA). The IEA group under implementing agreement for Advanced Materials for Transportation (AMT) identified thermoelectric material as an important area in 2009. The following is a report on international round-robin testing of transport properties of bulk thermoelectrics under IEA-AMT annex VIII.

2. International Round-Robin on Bulk Transport Properties

2.1 Background:

In the past 10 years, many progresses on thermoelectrics can be traced back to improvement in transport properties. In particular, materials with low thermal conductivity, high Seebeck coefficient and electrical conductivity have been developed to improve ZT. While many of the reports were in low dimensional materials, significant improvement has been made in bulk materials as well. The IEA-AMT efforts were focused on bulk materials because they have the greatest potential in automotive applications.

In bulk materials, the classic thermoelectric materials are: bismuth telluride [3] and lead telluride [5]. A new class of materials called skutterudites [7-13] emerged as an example of Glenn Slack's [7] perfect thermoelectric materials with the characteristics of phonon glass and electron crystal (PGEC). Other noticeable materials with high ZTs developed by various research groups are: clathrates [14-17], half heusler [18-28] alloys, TAGS [5, 29], LAST [30-32], β-Zn_3Sb_4 [33-42] and oxides [43-49].

These materials were among the top candidates for automotive applications since 2005. The first round of selection was based mainly on transport properties and figure of merit, ZT. During the selection process, some bulk materials were found unstable for high temperatures. The initial "good" properties could not be retained due to high temperature exposure. Other materials were found mechanically "unfit" to the thermal and mechanical cycling environment. For example, PbTe is the material used for Radioisotope Thermoelectric Generators (RTG) space probes for NASA [6]. It has been generating power successfully for more tens of years under a constant temperature gradient. However, the same materials were found damaged after several thermal cycles due to its mechanical strength and resistance to thermal shock. Unless the mechanical strength of PbTe is improved, it will not be suitable to automotive applications in which thousands of thermal cycles are expected during service.

Another important issue discovered in the past 6 years was the reliability of transport data. As the design and development of thermoelectric modules and devices are engineering processes in which the knowledge of transport properties is critical in the specification and ultimate performance of the thermoelectric devices. However, some of the materials with good figure of merit reported in the literature could not be reproduced or turned out to have much lower ZT than

expected. The participants in IEA-AMT annex VIII identified this issue in 2009 and started an international effort on transport properties through round-robin testing. In order to obtain the figure of merit, ZT, over the application temperature range, five separate measurements must be conducted:

1. thermal diffusivity (α in cm^2/sec)
2. specific heat (Cp in J/gK)
3. density (D in g/cm^3)
4. Seebeck coefficient (s in V/K)
5. electrical resistivity (ρ in Ohm-m)

The product of 1-3 gives thermal conductivity, $k = 100D\alpha Cp$ (in W/mK). Since density of the material is usually known or easy to measure, only four separate measurements are carried out to evaluate $ZT = s^2T/\rho k$. These multiple transport measurements can significantly influence the accuracy of ZT.

The initial round-robin study on n-type and p-type bismuth telluride was completed in May 2010. During the 2010 International Thermoelectric Conference in Shanghai China, the first annex meeting was held after the completion of first round-robin. It was clear that this timely effort by IEA-AMT is very important to the international thermoelectric community. The second round-robin study on p-type bismuth telluride was carried out and completed in August 2011.

2.2 Annex VIII Participants:

The IEA-AMT annex VIII was initiated in October 2009 and led Oak Ridge National Laboratories. Laboratories located in active IEA-AMT member countries are eligible to participate. Laboratories in non-IEA-AMT member countries who are interested in the effort were invited as observers. In particular, Japan and South Korea were observers and participated in the discussion and initial round-robin with the understanding that former membership would be required to be part of the annex VIII. Currently, the memberships of Japan and Korea are pending. Therefore, this report does not include them as formal participants. No data from these two countries are included in this report. Nine laboratories in 6 countries were involved in the 1st round-robin. Eventually, 9 laboratories in 4 member countries participated in the 2nd round-robin. The lead person in each laboratory is listed below:

- Dr. Hsin Wang, Oak Ridge National Laboratory, USA
- Professor Terry Tritt, Clemson University, USA
- Dr. Alex Mayolett, Corning Inc., USA
- Dr. Fred Harris, ZT-Plus Inc. USA
- Dr. Jeff Sharp, Marlow Industries, USA
- Dr. Jason Lo, CANMET, Canada
- Professor Holger Kleinke, University of Waterloo, Canada
- Professor Laszlo Kiss, University of Quebec at Chicoutimi, Quebec, Canada
- Professor Lidong Chen, Shanghai Institute of Ceramics, CAS, China
- Dr. Harold Bottner, Fraunhofer Institute for Physical Measurement Techniques, Germany

2.3 Selection of Bulk Thermoelectric Material

The most successful thermoelectric material to date is bismuth telluride. Thermoelectric cooling modules based on bismuth telluride have been produced in large quantities commercially. The largest US based thermoelectric materials and module producer is the Marlow Industries, located in Dallas TX. Two forms of bismuth telluride are made commercially by Marlow: 1) Bridgman materials which contain large oriented grains; 2) Micro Alloyed Materials (MAM) with small grain sizes and better uniformity. N-type and p-type MAM-like non-product materials made at Marlow with the best uniformity were selected for the round-robin study. The material selection criteria were not the best ZT, but the best uniformity and consistency.

In order to measure the four transport properties, multiple sets of 8 specimens of both n-type and p-type Bi_2Te_3 were prepared. Figure 1 is a picture of one set of IEA-AMT specimens.

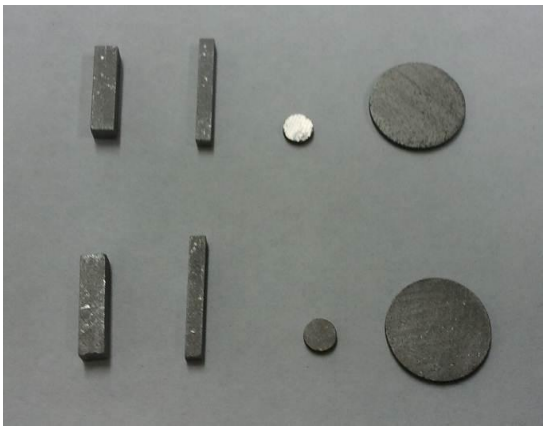

Figure 1. Round-robin 1 samples sent to each laboratory: 4 p-type (top row) and 4 n-type (bottom row) samples

The nominal composition of n-type material is $Bi_2Te_{2.7}Se_{0.3}$ and the nominal composition of p-type material is $Bi_{0.5}Sb_{1.5}Te_3$. The average grain size of the materials was about 20 μm. The specimens were prepared and machined to specifications by the Marlow Industries. A total of eight specimens prepared for transport properties testing were sent to each laboratory:

1) A set of 4 n-type bismuth telluride specimens

- A 4 mm diameter 1 mm thick disk for DSC measurement of Cp
- A 12.7 mm diameter 1mm thick disk for thermal diffusivity test
- A 2 mm x 2 mm x 15 mm bar for Seebeck coefficient and electrical resistivity tests
- A 3 mm x 3 mm x 12 mm bar for Seebeck coefficient and electrical resistivity tests

2) A set of 4 p-type bismuth telluride specimens

- A 4 mm diameter 1 mm thick disk for DSC measurement of Cp
- A 12.7 mm diameter 1mm thick disk for thermal diffusivity test
- A 2 mm x 2 mm x 15 mm bar for Seebeck coefficient and electrical resistivity tests
- A 3 mm x 3 mm x 12 mm bar for Seebeck coefficient and electrical resistivity tests

Each laboratory was asked to measure these samples to a maximum temperature of 225ºC starting from room temperature. Specifically, the following instructions were sent to each laboratory for testing:

1. *Seebeck coefficient from 50-225ºC*: Each lab needs to describe the equipment used (in-house or commercial system). Parameters to report: current electrode material, voltage/thermocouple type, test atmosphere. Measurement mode: set point with multiple delta T or temperature ramping. Analysis: Raw data and detailed analysis steps, corrections for probe Seebeck values.
2. *Electric resistivity from 50-225ºC:* Use the same specimen in Test 1. Parameter to report: current electrode material, voltage/thermocouple type, specimen dimensions, voltage probe distance, test atmosphere. Measurement mode: I-V test to confirm contact, ramping or set point mode, current reversal, if delta T exists during resistivity measurement. Analysis: how resistivity is determined at each temperature.
3. *Thermal diffusivity from 50-225ºC:* Use the 1 mm thick 12.7 mm diameter disk. Each lab needs to describe instrument used. Parameters to report: Sample thickness used, sample holder geometry and material. Measurements: record, test atmosphere, laser or flash lamp power, record raw transient. Analysis: Pulse width correction applied or not, calculation using Clark&Taylor, Koski or none-linear least-square curve fitting.
4. *Specific heat from 50-225ºC:* Use 4 mm diameter 1 mm thick disk. Each lab needs to describe equipment used. For DSC, parameters to report: sample weight, sample pan material, reference material (geometry and weight). Measurement: record raw data for empty pan (baseline), standard and test runs, specify test atmosphere, heating/cooling rate. Analysis: Cp calculation method.

3. International Round-Robin No. 1

One set of round-robin specimens were sent to each laboratory with instructions on temperature range. No guidelines for testing procedures were given and each laboratory was asked to perform the tests using their best practice. The following instruments were used by participating laboratories:

Seebeck coefficient and electrical resistivity:
- ULVAC ZEM-1, ZEM-2 and ZEM-3
- Modified Harman technique
- SRX (laboratory version)

Thermal diffusivity:
- Anter laser flash system
- Netszch laser flash system

Specific heat:
- Netzch DSC
- TA Instrument DSC

Not all the laboratories performed all the required tests due to limitation of instruments, especially in thermal diffusivity and specific heat measurements. All participating laboratories performed

Seebeck coefficient and electrical resistivity measurements. In the following discussion the laboratory identification numbers are not the same in each section. The lab identities were intentionally mixed because the main purpose is the round-robin was not to rank performance of each lab but rather to identify all the issues related to transport properties of bulk thermoelectrics.

3.1 Thermal diffusivity:

The thermal diffusivity results from 7 labs are shown in Figure 2. All the labs used the laser flash method. The two most common commercial systems made by Anter Corporation and Netzsch were used. The n-type materials are plotted in solid symbols and p-type materials are plotted in unfilled symbols with the same color. The raw data from each laboratory represented average values of at least three measurements at each temperature. The scatter at room temperature was about ±2-3% and the largest scatter of ±6% were at high temperatures for both p-type and n-type materials. The ASTM 1461 for flash diffusivity calls for the analysis using the Clark &Taylor method. The data analysis by each laboratory varied. Several laboratories used Cowan analysis. Since the original ASTM 1461 recommended limited number of data points to be used and most current software utilizes the entire curve to calculate diffusivity, a particular analysis was recommended to present the results. The overall results for thermal diffusivity were consistent among the 7 labs. Scatters in diffusivity values were expected given the measurement accuracy of commercial laser flash system is usually ±6-8%.

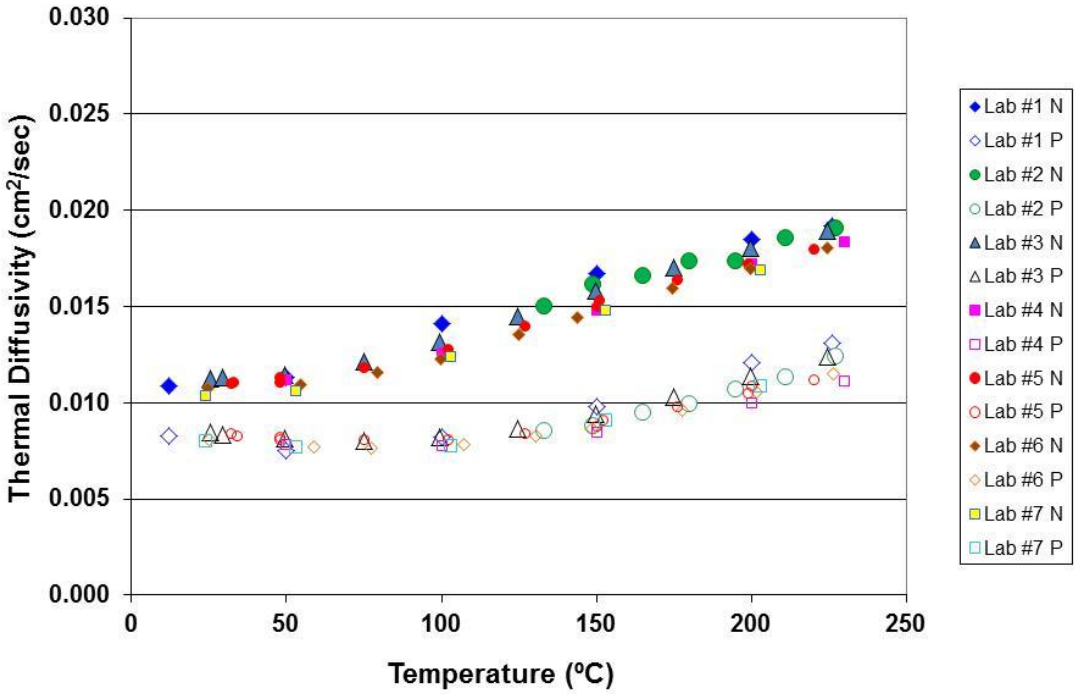

Figure 2. Thermal diffusivity results of round-robin 1 from 7 labs. n-type: filled symbols; p-type: unfilled symbols

3.2 Specific Heat:

The specific heat results from 6 labs are shown in Figure 3. All the labs used the differential scanning calorimeter (DSC) method. One lab performed the tests on two types of DSC and the heating and cooling data are both presented. It is clear the DSC measurements showed very large discrepancies among the labs. However, a closer look at the data indicated the data from two labs were obvious wrong and the remaining four labs showed reasonable good agreements.

The DSC method measures specific heat capacity under constant pressure, C_p. According to the theory for solids, C_p is slightly higher than C_v (heat capacity under constant volume). At temperature well above the Debye temperature, C_v can be approximated by the Dulong Petit limit 3NR, in which N is the number of atoms in the chemical composition of the material and R is a constant. In general, knowing the 3R= 24.9 J/molK and the molar mass of the material. C_v can be calculated. In DSC measurements, the Dulong Petit limit should be used as a guide line for the measured valued. Two basic rules need to be followed:

1) C_p should be a little higher than C_v
2) Due to thermal expansion, C_p should increase slightly at higher temperatures

For the two Marlow materials, Dulong Petit limit for the n-type materials is 0.159 J/gK and 0.186J/gK for the p-type material.

The DSC results from 6 labs showed the above two rules were not followed in some cases. One set of values were too low (Lab #1) and another set (Lab #3) of values were too high. These results showed 40-50% or even higher than expected C_p values, and the materials must be re-measured. Usually, when the proper procedures are not followed, the DSC results can be erroneous. The most important thing to check is heating and cooling curves. If the two curves are not repeatable it is an

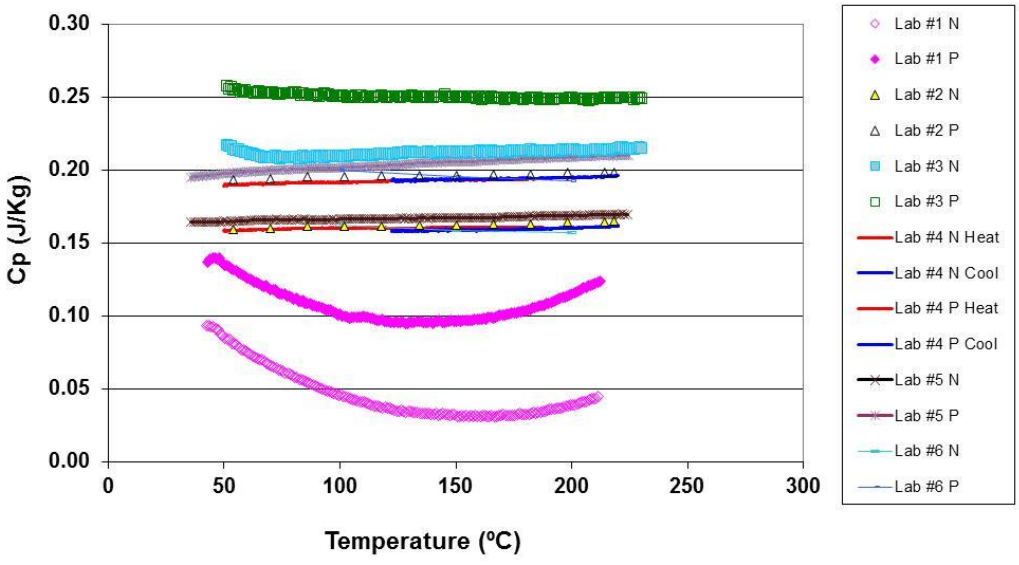

Figure 3. Specific heat capacity results of round-robin 1 from 6 labs.

indication of instrument baseline shift. A new baseline must be run in order to obtain correct C_p values. When the C_p data from Lab #1 and #3 are removed in Figure 3, the scatted among other sets of data were about ±4%. After the first round-robin, a document was prepared for DSC operators to fill out and answer. It is a step towards developing standard procedures in Appendix A.

3.3 Seebeck Coefficient:

Seebeck coefficient results from 7 labs and Marlow are shown in Figure 4. Three different types of instruments were used. The values for both n-type and p-type materials indicated the Seebeck measurements produced consistent results among the participating labs. Among labs using ULVAC ZEM system the scatter was about ±4% for the short and long specimens. When the other two techniques are included the scatter became about ±5.5%. The major difference comes from contact location and where temperature and voltage are measured. The ULVAC ZEM systems (4-probes) seem to give a slightly higher absolute Seebeck value. The system using end contacts gave a slightly low Seebeck value. The Marlow data obtained by modified Harman method seem to be a good compromise, although it only measured data up to 75ºC. The other source of error in Seebeck

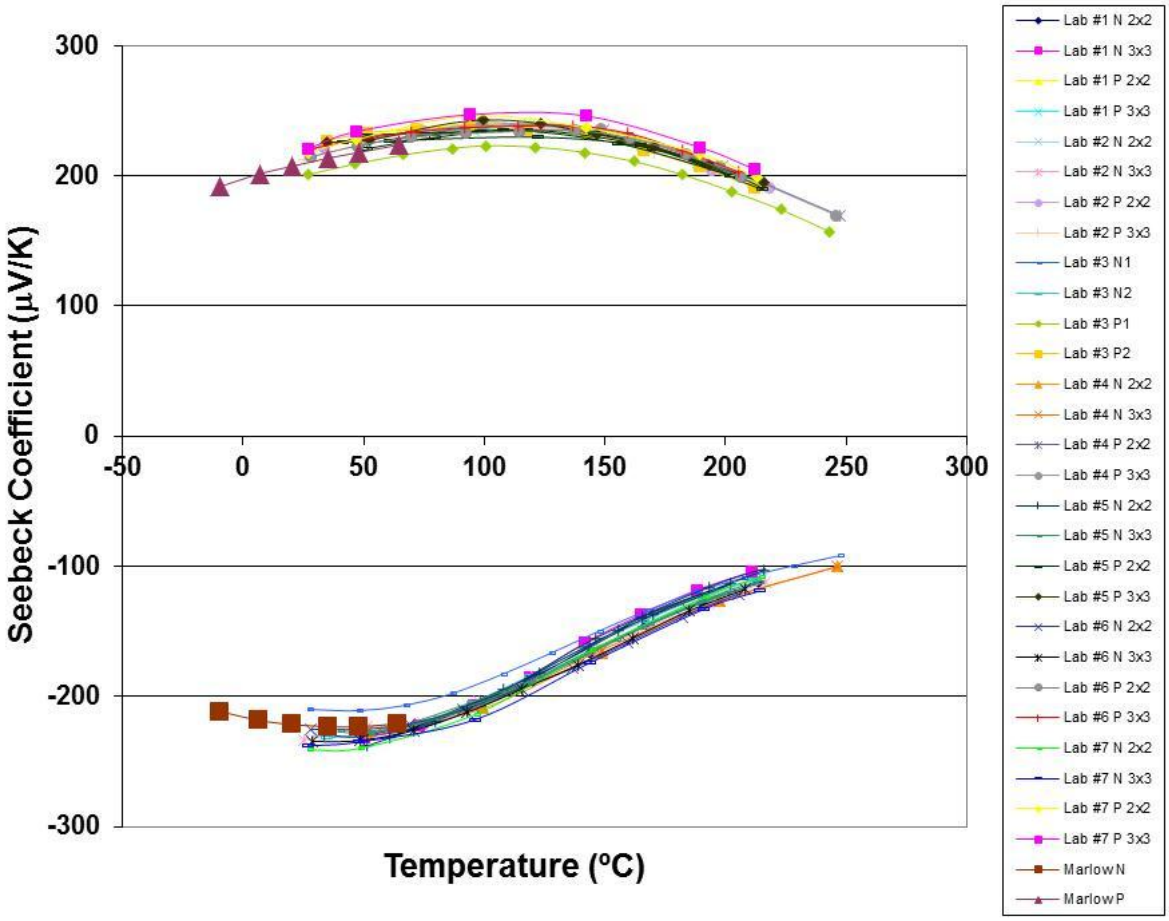

Figure 4. Seebeck coefficient results of round-robin 1 from 7 labs and Marlow

measurements may come from the probe calibration. A correction value is needed to calculate Seebeck coefficient as the probes are part of the measurement loop. Knowing the correct calibration value determines the measurement accuracy. However, the probe Seebeck values could change after high temperature exposures, especially when inter-diffusion between the probe tips and thermoelectrics occur. The standard materials (Constatan for ULVAC ZEM system) need to be periodically examined.

3.4 Electrical Resistivity:

Electrical resistivity results from 7 labs and Marlow are shown in Figure 5. Similar to Seebeck coefficient, three different types of instruments were used as these two properties are normally measured on the same specimen using the same probes. The resistivity results showed much larger scatter for both p-type and n-type specimens. The largest scatter for n-type material near 100ºC was about ±12.5%. The scatter for the p-type material was smaller, although it seemed to be more scattered at high temperatures. There was no clear difference between the short (3x3x12 mm^3) samples and long (2x2x15 mm^3) samples. However, the most significant errors were identified to come from the measurement and determination of probe distance. In some early ZEM systems the probe distance was not measured every time. Since the probe size is about 0.5 mm, it could easily introduce a 10% error in a measurement when the probe spacing is 5 mm. In the current version of ULVAC ZEM-3, a digital microscope is used to accurately measure the probe distance. The main source of error for electrical resistivity is the uncertainty of geometry measurements.

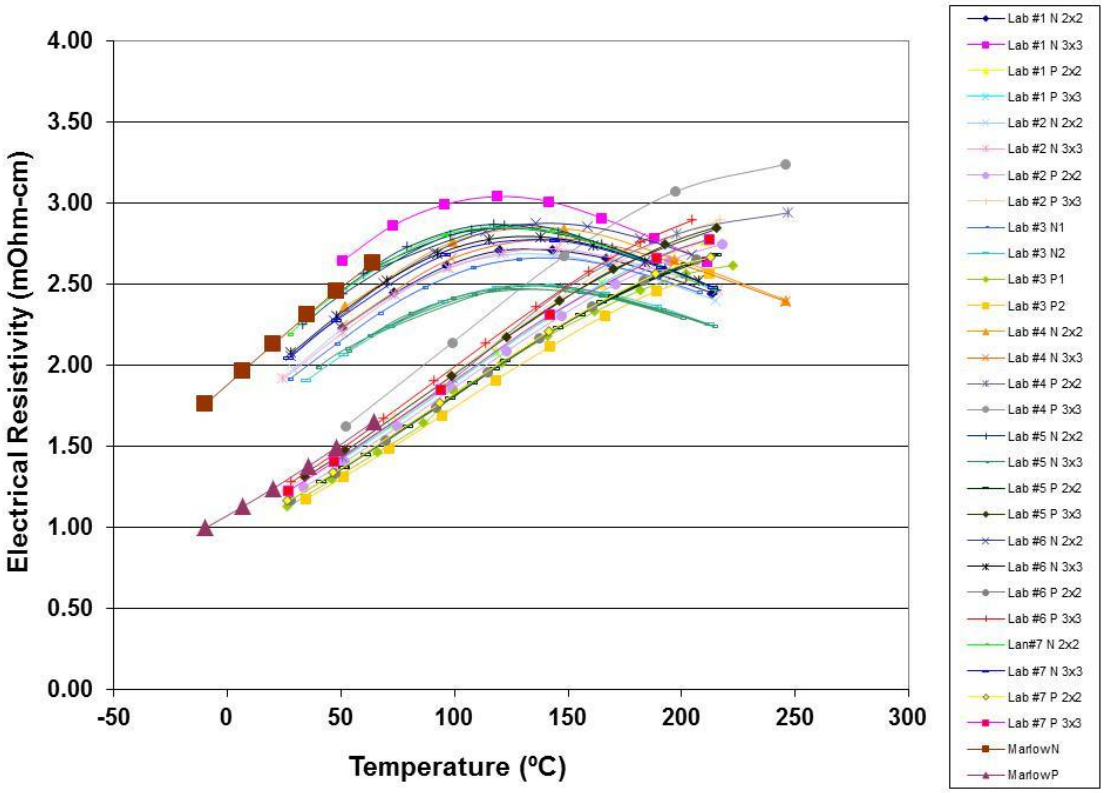

Figure 5. Electrical resistivity results of round-robin 1 from 7 labs and Marlow

3.5 Summary of Round-Robin 1:

The first round-robin among 7 laboratories using the Marlow Bi_2Te_3 was completed within 4 months. The study achieved its original goal, i.e. to identify measurement problems for bulk transport properties measurements. Using the commercially available materials and moderate temperature range, the IEA-AMT annex study observed the following:

1. Thermal diffusivity measurements by laser flash give about ±6% errors. The test results could be better if the ASTM 4161 data analysis procedure is followed.
2. Specific heat measurements show a huge scatter. It seems to be the most difficult test although ASTM standard exist for the DSC method. The largest errors occur when the baseline of the instrument is shifted during reference, empty pan and sample runs. When obvious mistakes are eliminated the measured Cp data showed an error of ±4%.
3. Seebeck coefficient measurements showed very good agreement among the labs. The measurement errors were about ±5.5% for both types of materials and two geometries.
4. Electrical resistivity measurements of both p-type and n-type materials showed large errors. The largest error ±12.5% occurred for the n-type material near 100ºC. The uncertainty for dimension measurements was identified as the main source of error.

The round 1 test used Marlow MAM materials. Although it is known to have consistent properties, it is still possible to have scatter due to localized material non-uniformity. Since each lab received a separate set of specimens, the possibility of errors caused of materials did exist. In order to understand the materials uniformity, groups of 12 n-type and p-type Marlow materials were selected and tested at room temperature.

Figure 6 shows room temperature thermal diffusivity results of 12 n-type and 12 p-type samples.

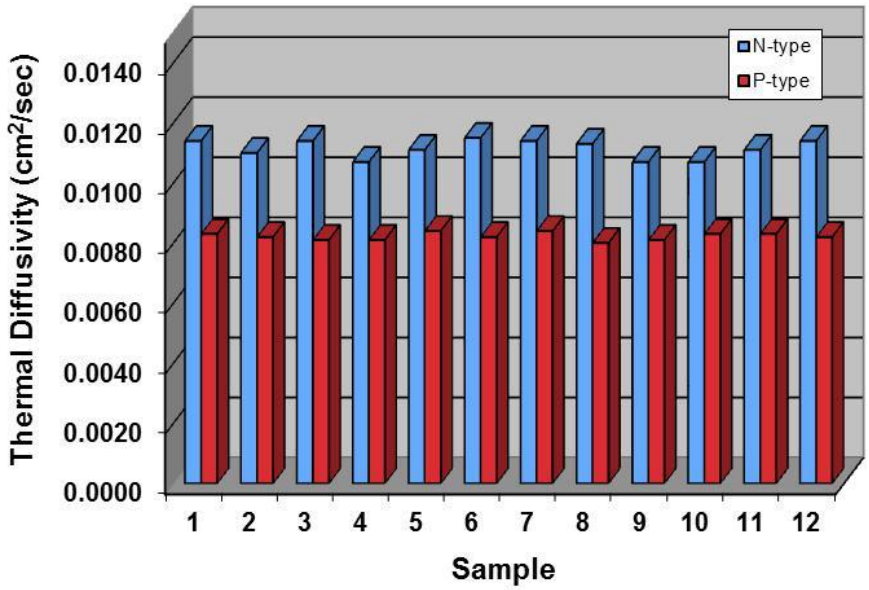

Figure 6. Thermal diffusivity of 12 n-type and 12 p-type samples at room temperature

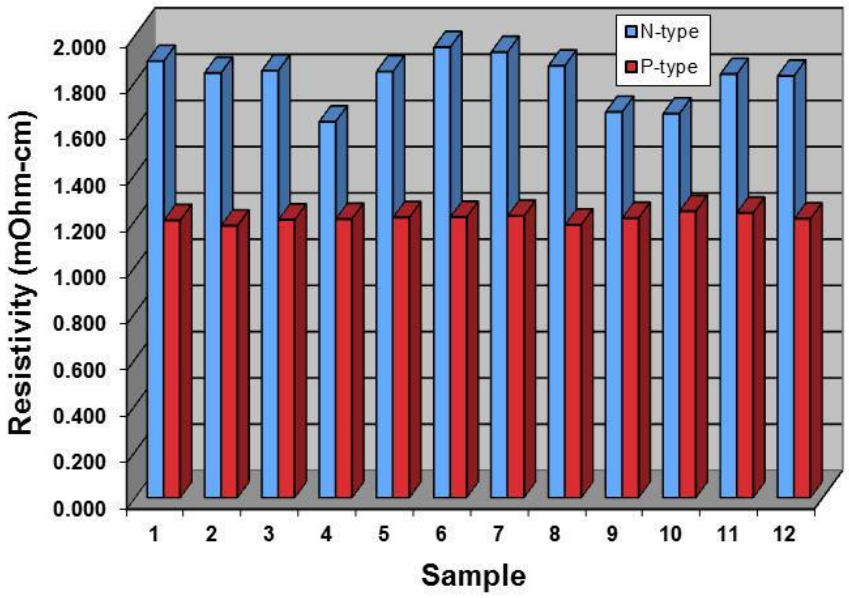

Figure 7. Electrical resistivity of 12 n-type and 12 p-type samples at room temperature

The specimens are 12.7mm diameter, 1mm thick disks from the same batch of IEA-AMT round robin materials. An Anter X-platform xenon flash system was used. The room temperature system has a 24-sample carousel and uses an intrinsic contact thermocouple to detect temperature rise. As shown in Figure 6, the standard deviations were $\pm$1.54% for p-type materials and $\pm$2.75% for the n-type materials.

Figure 7 shows room temperature electrical resistivity results of 12 n-type and 12 p-type samples. The specimens are the same 12.7mm diameter 1mm thick disks for thermal diffusivity measurements. A 4-point in-line probe station by Signatone was used. As shown in Figure 7, the standard deviations were $\pm$1.50% for p-type materials and $\pm$5.81% for the n-type materials.

Based on the above results, the n-type material showed larger sample-to-sample variations in thermal diffusivity and electrical resistivity. This could have contributed to the measurement errors in round-robin 1, especially in the electrical resistivity results. It was determined by the annex participants to conduct a second round-robin using the p-type materials.

4. International Round-Robin No. 2

The second round-robin testing began in August of 2010 and was completed by August 2011. Two sets of p-type materials were measured at 7 labs in 4 countries. The results of round-robin 1 were given to all the labs as reference. The issues identified in round-robin 1 were discussed by participating labs. The same test instruments used for round-robin 1 were used for all the transport properties in round-robin 2. All the labs completed tests on all specimens. In some cases, thermal and electrical properties testing were carried out at different labs within the same country.

4.1 Thermal diffusivity:

The thermal diffusivity results from 7 labs are shown in Figure 8. All the labs used the laser flash system made by either the Anter Corporation or Netzsch. The two p-type specimens were measured separately in some cases a few months apart. Except for one measurement by Lab #6, the scatter at room temperature was about ±4% and the largest scatters of ±10% were observed at 200ºC. Larger scatters occurred comparing to round-robin 1. Since the same materials were passed around, the differences results from sample-to-sample variations were minimized. One lab used a cryogenic temperature system to measure the diffusivity down to -150ºC. The data agreed well with the lab averages, and it gave a better idea on the trend of diffusivity vs. temperature. Detailed data analysis is being conducted to understand how the data were generated and processed. We expect to discover measurement and data analysis issues that led to the larger scatter and an operating procedure for thermal diffusivity measurement will be generated.

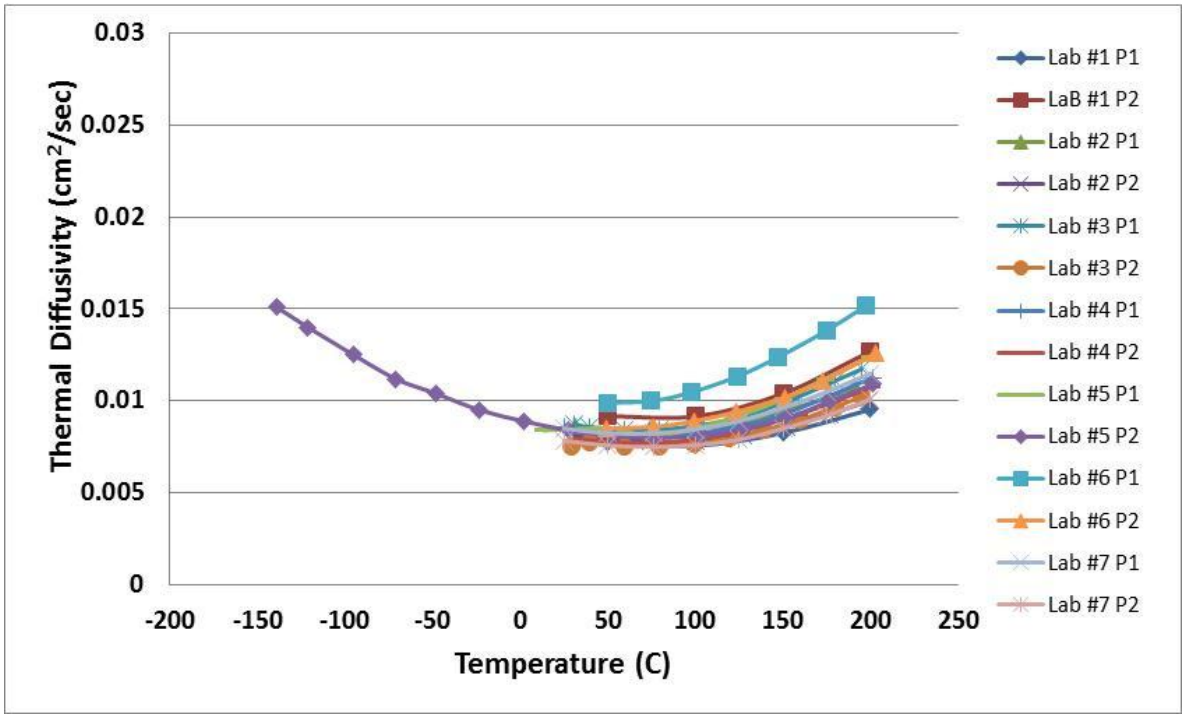

Figure 8. Thermal diffusivity results of round-robin 2 from 7 labs.

4.2 Specific Heat:

The specific heat results from 7 labs are shown in Figure 9. Although specific guide lines were sent to the labs, DSC measurements continued to present the biggest challenge. More than ±15% scatter were observed in the combined data. In most cases, the test procedure was followed. However, the nature of DSC measurements, i.e. three separate runs must be taken to calculate Cp, made this test the most difficult one to be reproducible. In the most common DSC systems, the baseline change is a fact and cannot be controlled by the operator. The best practice is to run a baseline and reference run, record heating and cooling data on test specimen and run the baseline again. If shifts are found, the Cp calculations need to use the correct baseline values. If the baseline shifts too much, the test has to be repeated. A common standard for DSC is a molybdenum specimen from NIST. The Cp should be run against the NIST standard to periodically check the accuracy of the instrument. In some cases, the variation can be identified. For example, the results from Lab#2 in Figure 2 showed significant "hook" in the beginning of the run. This is usually caused by a mismatch in mass or size of the reference sample. The reference sample should match the test sample in mass and shape as close as possible. There were also two cases of uncorrected baseline shifts that resulted in larger deviations from the Dolung Petit limit of 0.186 J/gK for the p-type material.

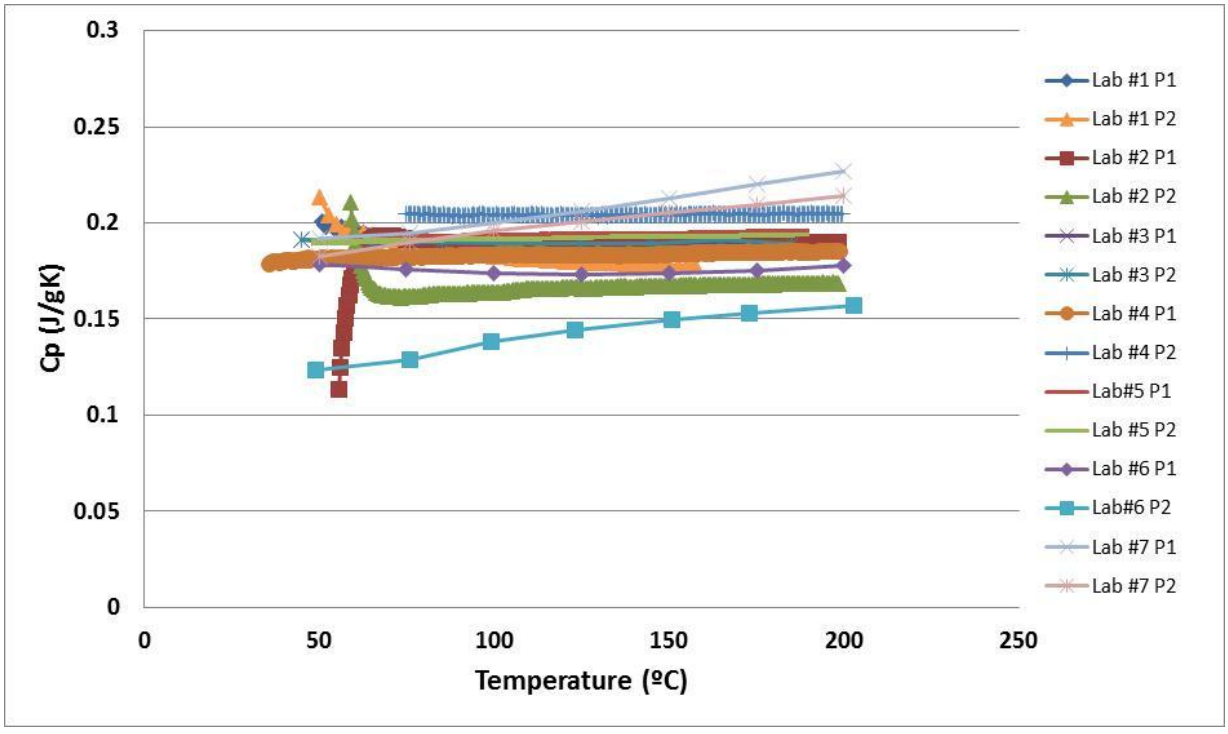

Figure 9. Specific heat results of round-robin 2 from 7 labs.

4.3 Seebeck Coefficient:

Seebeck coefficient results from 7 labs and Marlow are shown in Figure 10. Similar to round-robin 1, the agreements in Seebeck measurements were much better than other properties. All 7 labs used ULVAC ZEM systems. One lab also ran the test using a lab-made system which used a different contact mechanism. The Marlow data was obtained using modified Harman method on a 4 x 4 x 5 mm^3 specimen. For all the ULVAC ZEM results, the scatter was about $\pm$4% in the entire temperature range. The end-contact method gave lower Seebeck values. The Marlow Seebeck values lay in between the ULVAC values and End-contact values. Because of the size of the probes in ULVAC system it is possible to over-estimate the Seebeck values. On the other hand, the end-contact method could be underestimating the Seebeck values. No large variations were observed in the Seebeck coefficient results.

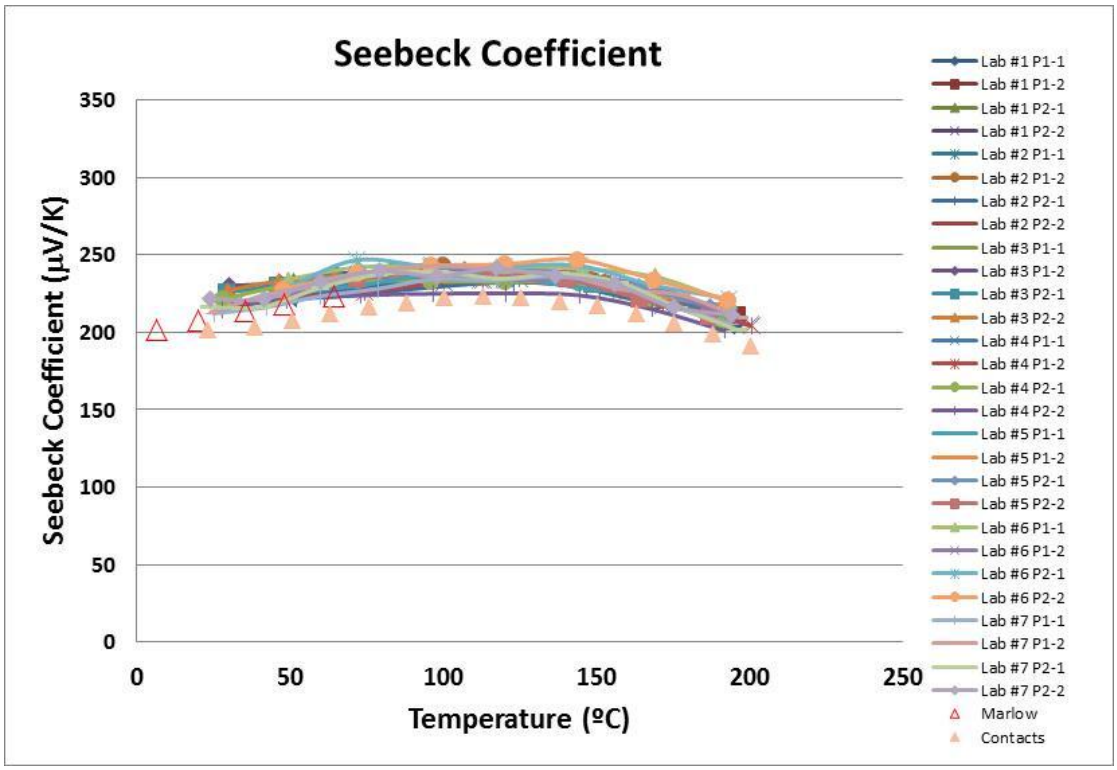

Figure 10. Seebeck coefficient results of round-robin 2 from 7 labs and Marlow.

4.4 Electrical Resistivity:

Electrical resistivity results from 7 labs and Marlow are shown in Figure 11. All the data were obtained from simultaneous measurements with Seebeck coefficient. Each lab measure a long (2 2 x 15 mm^3) sample and a short sample (3 x 3 x 12 mm^3) for each set. The scatter was about $\pm$5% near room temperature and increased to about $\pm$9% at 200ºC. A total of 4 specimens were measured by each lab. Not all the ZEM system were equipped with digital probe spacing measurements features. Errors introduced by geometry measurements still exist. However, the increasing scatter at higher

temperatures indicated the measurements and data analysis have not been optimized. The Marlow data showed very good agreement with the round-robin results up to 75ºC.

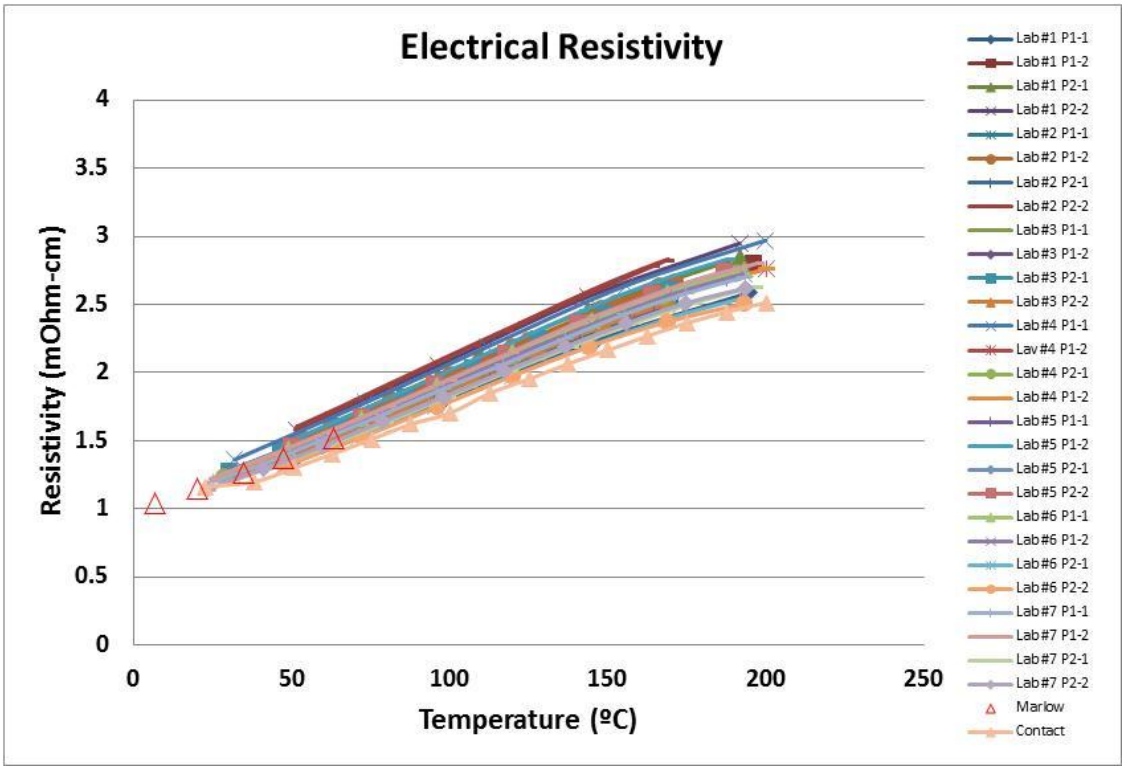

Figure 11. Electrical resistivity results of round-robin 2 from 7 labs and Marlow.

4.5 Summary of Round-Robin 2:

The second round-robin among 7 laboratories using the Marlow Bi_2Te_3 was completed within 12 months. By measuring the same specimens, the differences introduced by sample-to-sample variations were minimized. However, measurement issues still existed. In some cases the data showed larger scatter than the first round-robin. In general, we found:

1. Thermal diffusivity of p-type materials showed $\pm$4% scatter at room temperature and $\pm$10% scatter at 200ºC (except for one sample from one lab).
2. Specific heat showed more than $\pm$15% scatter in the temperature range. Half of the labs could measure within 4-5% of the Dulong Petit limit. Results from some labs still show lack of checking with standard or uncorrected baseline shifts.
3. Seebeck coefficient showed good agreement and about $\pm$4% scatter over the entire temperature range. Results using another contact method indicated the possibility of systematic error of a few percent.
4. Electrical resistivity results showed better agreement than round-robin 1. The room temperature scatter was about $\pm$5%, and it increased to $\pm$9% at 200ºC.

5. Conclusions

Two international round-robin studies were conducted on transport properties measurements of bulk thermoelectric materials. The study discovered current measurement problems. In order to get ZT of a material, four separate transport measurements must be taken. The round-robin study showed that among the four properties, Seebeck coefficient is the one that can be measured consistently. Electrical resistivity has $\pm$4-9% scatter. Thermal diffusivity has similar $\pm$5-10% scatter. The reliability of the above three properties can be improved by standardizing test procedures and enforcing system calibrations. The worst problem was found in specific heat measurements using DSC. The probability of making measurement error is great due to the fact that three separate runs must be taken to determine Cp, and the baseline shift is always an issue for commercial DSC. It is suggested the Dulong Petit limit be always used as a guideline for Cp. Procedures have been developed to eliminate operator and system errors. The IEA-AMT annex has developed standard procedures for transport properties testing. The preliminary procedures are shown in Appendix A.

ACKNOWLEDGEMENT

The authors would like to thank the support of the International Energy Agency (IEA) and the Implementing Agreement on Advanced Materials for Transportation (AMT). Special thanks to AMT chairman, Jerry Gibbs (DOE), and vice chairman, Stephen Hsu (George Washington University), and all members of the IEA-AMT executive committee (ExCo) for their guidance to Annex VIII.

Most laboratories participated voluntarily and contributed time and resources to the project.

In Canada, we thank the support of CANMET and special thanks to Jenifer Jackman and Weuyue Zheng for ExCo reviews and guidance. Jason Lo is the project leader and he would like to thank supports from Holger Kleinke (University of Waterloo) and Laszlo Kiss (University of Quebec at Chicoutimi) on performing measurements.

In China, we thank the support of the Shanghai Institute of Ceramics under the Chinese Academy of Sciences. Lidong Chen and Shengqiang Bai would like to than, Xun Shi and Wenqing Zhang of SICCAS for their contributions.

In Germany, we thank Juergen Lexow of BAM for his support at ExCo. Harold Bottner and Jan Konig would like to thank the support from Fraunhofer Institute for Physical Measurement Techniques.

In the USA, we thank the financial support of US Department of Energy, the High Temperature Materials Laboratory user program at Oak Ridge National Laboratory managed by UT-Battelle LLC. We also want thank the support of the Marlow Industries, Clemson University, ZT-PLUS, Corning Inc.

REFERENCES

1. A.F. Ioffe, *Semiconductor Thermoelements and Thermoelectric Cooling* (Infosearch, London,1957).
2. J.C. Peltier, *Ann. Chem.* **LVI** (1834) p. 371.
3. H.J. Goldsmid, *Electronic Refrigeration* (Pion Limited, London, 1986).
4. D.M. Rowe, ed., *CRC Handbook of Thermoelectrics* (CRC Press, Boca Raton, FL, 1995).
5. G.S. Nolas, J. Sharp, and H.J. Goldsmid, *Thermoelectrics: Basic Principles and New Materials Developments* (Springer, New York, 2001).
6. Jet Propulsion Laboratory Thermoelectric Science and Engineering Web site, http://www.its.caltech.edu/_jsnyder/thermoelectrics/(accessed February 2006).
7. G. A. Slack, in *CRC Handbook of Thermoelectrics,* edited by D. M. Rowe (CRC, Boca Raton, FL, 1995), pp. 407.
8. G. S. Nolas, G. A. Slack, and S. B. Schujman, Semicond. Semimet. **69**, 255 (2000).
9. B. C. Sales, D. Mandrus, and R. K. Williams, Science **272**, 1325 (1996).
10. B. C. Sales, D. G. Mandrus, and B. C. Chakoumakos, Semicond. Semimet. **70**, 1 (2001).
11. D. T. Morelli and G. P. Meisner, J. Appl. Phys. **77**, 3777 (1995).
12. C. Uher, Semicond. Semimet. **69**, 139 (2000).
13. C. Keppens *et al.*, Nature **395**, 876 (1998).
14. V.L. Kuznetsov, L.A. Kuznetsova, A.E. Kaliazin, and D.M. Rowe, *J. Appl. Phys.* **87** (2000) p. 7871.
15. G.S. Nolas, *Thermoelectrics Handbook:Macro- to Nano-Structured Materials*, edited by D.M. Rowe (CRC Press, Boca Raton, FL) in press.
16. W. Jeischko, *Metall. Trans. A* **1** (1970) p. 3159.
17. S.J. Poon, in *Recent Trends in Thermoelectric Materials Research II,* edited by T.M. Tritt, *Semiconductors and Semimetals,* Vol. 70, Chap. 2, treatise editors, R.K. Willardson and E.R. Weber (Academic Press, New York, 2001) p. 37.
18. J. Tobola, J. Pierre, S. Kaprzyk, R.V. Skolozdra, and M.A. Kouacou, *J. Phys. Condens. Matter* **10** (1998) p. 1013.
19. F.G. Aliev, N.B. Brandt, V.V. Moschalkov, V.V. Kozyrkov, R.V. Scolozdra, and A.I. Belogorokhov, *Phys. B: Condens. Matter* **75** (1989) p. 167.
20. S. Ogut and K.M. Rabe, *Phys. Rev. B* **51** (1995) p. 10443.
21. W.E. Pickett and J.S. Moodera, *Phys. Today* **54** (2001) p. 39.
22. C. Uher, J. Yang, S. Hu, D.T. Morelli, and G.P. Meisner, *Phys. Rev. B* **59** (1999) p. 8615.
23. H. Hohl, A.P. Ramirez, C. Goldmann, G. Ernst, B. Wolfing, and E. Bucher, *J. Phys. Condens. Matter* **11** (1999) p. 1697.
24. S. Sportouch, P. Larson, M. Bastea, P. Brazis, J. Ireland, C.R. Kannenwurf, S.D. Mahanti, C. Uher, and M.G. Kanatzidis, in *Thermoelectric Materials 1998—The Next Generation Materials for Small-Scale Refrigeration and Power Generation Applications*, edited by T.M. Tritt, M.G. Kanatzidis, G.D. Mahan, and H.B. Lyon Jr. (*Mater. Res. Soc. Symp. Proc.* **545**, Warrendale, PA, 1999) p. 421.

25. S. Bhattacharya, A.L. Pope, R.T. Littleton IV, T.M. Tritt, V. Ponnambalam, Y. Xia, and S.J. Poon, *Appl. Phys. Lett.* **77** (2000) p. 2476.
26. Y. Xia, S. Bhattacharya, V. Ponnambalam, A.L. Pope, S.J. Poon, and T.M. Tritt, *J. Appl. Phys.* **88** (2000) p. 1952.
27. Q. Shen, L. Chen, T. Goto, T. Hirai, J. Yang, G.P. Meisner, and C. Uher, *Appl. Phys. Lett.* **79** (2001) p. 4165.
28. S. Sakurada and N. Shutoh, *Appl. Phys. Lett.* **86** (2005) p. 2105.
29. E. Skrabeck and D.S. Trimmer, in *CRC Handbook of Thermoelectrics*, edited by D.M. Rowe (CRC Press, Boca Raton, FL, 1995) p. 267. 49. R.
30. K.F. Hsu, S. Loo, F. Guo, W. Chen, J.S. Dyck, C. Uher, T. Hogan, E.K. Polychroniadis, and M.G. Kanatzidis, *Science* **303** (2004) p. 818.
31. S. Sportouch, M. Bastea, P. Brazis, J. Ireland, C.R. Kannewurf, C. Uher, and M.G. Kanatzidis, in *Thermoelectric Materials 1998—The Next Generation Materials for Small-Scale Refrigeration and Power Generation Applications*, edited by T.M. Tritt, M.G. Kanatzidis, G.D. Mahan, and H.B. Lyon Jr. (*Mater. Res. Soc. Symp. Proc.* **545**, Warrendale, PA, 1999) p. 123.
32. E. Quarez, K.F. Hsu, R. Pcionek, N. Frangis, E.K. Polychroniadis, and M.G. Kanatzidis, *J. Amer. Chem. Soc.* **127** (2005) p. 9177.
33. H.W. Mayer, I. Mikhail, and K. Schubert, *J. Less-Common Metals* **59** (1978) p. 43.
34. T. Caillat, J.-P. Fleurial, and A. Borshchevsky, *J. Phys. Chem. Solids* **58** (1997) p. 1119.
35. V.L. Kuznetsov and D.M. Rowe, *J. Alloys Compd.* **372** (2004) p. 103.
36. S.C. Ur, I.H. Kim, and P. Nash, *Mater. Lett.* **58** (2004) p. 2132.
37. K. Ueno, A. Yamamoto, T. Noguchi, T. Inoue, S. Sodeoka, H. Takazawa, C.H. Lee, and H. Obara, *J. Alloys Compd.* **385** (2004) p. 254.
38. G.J. Snyder, M. Christensen, E. Nishibori, T. Caillat, and B.B. Iversen, *Nature Mater.* **3** (2004) p. 458.
39. M. Tsutsui, L.T. Zhang, K. Ito, and M. Yamaguchi, *Intermetallics* **12** (2004) p. 809.
40. F. Cargnoni, E. Nishibori, P. Rabiller, L. Bertini, G.J. Snyder, M. Christensen, and B.B. Inversen, *Chem. Eur. J.* **20** (2004) p. 3861.
41. S.G. Kim, I.I. Mazin, and D.J. Singh, *Phys. Rev. B* **57** (1998) p. 6199.
42. J. Nylen, M. Andersson, S. Lidin, and U. Haeussermann, *J. Am. Chem. Soc.* **126** (2004) p. 16306
43. I. Terasaki, Y. Sasago, and K. Uchinokura, *Phys. Rev. B* **56** (1997) p. R12685.
44. R. Funahashi, I. Matsubara, H. Ikuta, T. Takeuchi, U. Mizutani, and S. Sodeoka, *Jpn. J. Appl. Phys. Pt. 2* **39** (2000) p. L1127.
45. A.C. Masset, C. Michel, A. Maignan, M. Hervieu, O. Toulemonde, F. Studer, B. Raveau, and J. Hejtmanek, *Phys. Rev. B* **62** (2000) p. 166.
46. Y. Miyazaki, K. Kudo, M. Akoshima, Y. Ono, Y. Koike, and T. Kajitani, *Jpn. J. Appl. Phys. Pt. 2* **39** (2000) p. L531.
47. A. Satake, H. Tanaka, T. Ohkawa, T. Fujii, and I. Terasaki, *J. Appl. Phys.* **96** (2004) p. 931.
48. M. Shikano and R. Funahashi, *Appl. Phys. Lett.* **82** (2003) p. 1851.
49. I. Matsubara, R. Funahashi, T. Takeuchi, S. Sodeoka, T. Shimizu, and K. Ueno, *Appl. Phys. Lett.* **78** (2001) p. 362

Appendix A

IEA-AMT Thermoelectric Transport Properties Testing Procedure

Appendix A

IEA-AMT Thermoelectric Transport Properties Testing Procedure

The following is the current test procedures of bulk thermoelectric for the purpose of evaluating the figure of merit, ZT. The procedures will be further modified as more round-robin tests and analysis are conducted.

For bulk materials, five separate measurements need be conducted:

1. thermal diffusivity (α in cm^2/sec)
2. specific heat (Cp in J/gK)
3. density (D in g/cm^3)
4. Seebeck coefficient (s in V/K)
5. electrical resistivity (Ohm-m)

The product of thermal diffusivity, specific heat and density gives thermal conductivity:

$$k = 100D\alpha Cp \quad (W/mK)$$

The figure of merit ZT is calculated using:

$$ZT = s^2T/\rho k$$

where T is temperature in Kelvin (K).

1. Test procedure for thermal diffusivity:

Specimen: The standard thermal diffusivity specimen should be a thin disk or plate. For most commercial equipment the standard specimen geometry is a 12.7 mm diameter disk. The thickness for the disk is determined by the thermal diffusivity values of the material. In general, the diameter of the specimen should be at least 4-5 times larger than the thickness. This is to ensure the one-dimensional heat flow assumption is valid. If the thickness is comparable to the diameter, heat loss from the side of the specimen will cause measurement errors. For thermoelectric with thermal conductivity of 1-3 W/mK, the thickness of the specimen is usually 1-2 mm.

To prepare the specimen the most important thing is to keep a parallel surface since the thickness is the only parameter to be entered during thermal diffusivity test. The accuracy of the thickness will directly affect the accuracy of the thermal diffusivity. The surfaces need to be flat. Polishing is not required. Mirror-like surface finish will reflect heat pulse (laser or xenon flash light) and present low emissivity for the infrared detectors. To ensure consistent surface conditions, it is a common practice to spray a thin layer of graphite on both side of the specimen. For materials that are

translucent or transparent, a thin layer of metal coating (or graphite coating) is required. The commercial laser flash system usually employs a YAG laser (1.06 μm wavelength) and InSb infrared detector (3-5 μm). It is important to make sure the specimen is not transparent in these IR wavelengths. An example is silicon, which is highly transparent in the IR region. In this case, metal or graphite coating is required.

Thermal diffusivity test: Thermal diffusivity test is a time-domain transient method. There is no need to measure specimen temperature, as long as the temperature rise of the specimen is small. The half-rise time, i.e. the time to reach half-maximum temperature (expressed in detector voltage) is measured from the back of the specimen.

Laser power: The laser power should be enough to raise the back surface temperature 1-5ºC. In general, 1-2V from the IR detector with low noise is sufficient. In some systems, the laser power can be adjusted by the software. It is important to know the IR detector response is not sensitive at room temperature, but its sensitivity increases exponentially as temperature increases.

Data collection time: The commercial systems either collect data for a fixed length of time (12 seconds) or try to adjust optimal data collection time after determine the peak position following the first shot. It is usually the rule-of-thumb to keep the time to reach peak within two seconds after the heat pulse. If it takes long than two seconds to reach maximum temperature, it usually an indication that the specimen could be thinner. For low thermal conductivity materials, it is important to wait sufficient long time in between heat pulses to allow the specimen to cool down.

Number of measurements: Usually at least 3 measurements are need for each specimen at each set point.

Calibration and references: In order, to calibrate the flash diffusivity system several standards are used such as Poco graphite or thermal graphite, Pyroceram 9606, PYREX, stainless steel or alumina. For thermoelectric materials, Pyroceram 9606 which has similar thermal diffusivity and thermal conductivity should be used. If it is not available stainless steel or alumina references can be used. Calibration runs (or periodic calibration runs) are necessary to show the system is operating within designed specification when the test is performed.

Data analysis: Thermal diffusivity calculation is based on one-dimensional heat flow model. The simplest calculation is under the adiabatic condition, i.e. the Parker method:

$$\alpha = 0.138\ d^2/t_{0.5}$$

where d is the specimen thickness and $t_{0.5}$ is the time to reach half maximum. In reality, the specimen will have heat loss and the laser of xenon flash pulse width needs to be corrected. In the ASTM 1461 for the flash method, the calculation to correct the Parker equation is recommended. These methods are mainly corrections of the constant in the Parker equation. The ASTM 1461 recommends the Clark and Taylor (ratio method) and the Cowan methods. Other calculation methods such as, radiation method, the Koski method, Heckman and Cape and Lehman are frequently used. These methods were developed for specific materials or specific conditions. When

using each method, it is important to understand the specific conditions that apply to the method, i.e. very high or low thermal conductivity, transparent materials or inhomogeneous materials. For thermoelectrics with thermal conductivity of 1-5 W/mK and opaque in the visible and IR range, it is the advice of IEA-AMT to use the Clark and Taylor or Cowan method suggested in the ASTM 1461.

Reporting: Thermal diffusivity values calculated by Clark and Taylor or Cowan method need to be reported. The specimen geometry, laser power and data collection time need to be specified. Diffusivity data from multiple tests should be report and standard deviation can be calculated to show repeatability. Test results of periodic calibration of the system using reference materials need to be available. The raw transient data need to be examined for signal quality and saved for future analysis.

2. Test procedure for specific heat:

Specimen: The standard specific specimen for differential scanning colorimeter (DSC) should be a thin disk, 4-6 mm in diameter and about 1 mm thick depending on the measurement system selected. The specimen needs to be flat and have the mass close the reference material. Powders, broken pieces or specimen have different geometry will have different heat transfer characteristics from the reference material and introduce measurement errors. Descriptions of specimen holders/pans/lids including material, geometry, dimensions, mass, and venting or sealing type needed to be recorded.

DSC measurements and data analysis: The DSC method to determine specific heat is described in ASTM standard E1296 and ISO 11357. The test requires three separate scans: an empty pan (baseline scan); a scan using sapphire standard; and a sample scan. A typical DSC test should include a heating scan and a cooling scan. It is highly recommended to run another baseline scan after the test, especially when the heat and cooling curves show significant shifts.

When performing the DSC measurements and data analysis the following steps need to be followed:

1. Select the calorimeter mode: DSC-Standard Ramp, DSC-Step, DSC-Modulated Ramp, DSC-Modulated Quasi-isothermal, or other.
2. Specify sensor Type/Model and provide a description (include diagram) of sensor thermocouple placement, type (separate- 4 wire, differential- 3 wire, thermopile, etc.) and thermocouple material
3. Description of data analysis software including name and version number. If any baseline drift corrections were used please describe algorithm used:
4. Description of pre-test procedure including vacuum/purge cycles, vacuum bake out/degassing, purge gas type, purity and flow rate. If sealed lids were used, include atmosphere conditions pans were sealed under.
5. Description of standard reference material used for heat flow calibration including material, geometry, dimensions, mass, and any traceability to a national standards organization. Include a text file of the heat capacity vs. temperature values for the

material used.

6. Description of test procedure including any standard test method followed (ASTM, ISO, DIN, etc), starting and ending temperatures, temperature and duration of any isothermal segments, heating/cooling rates used, and period and amplitude if using modulated techniques. Please note specifically if a "single run" method using a stored instrument calorimetric calibration was used to calculate the heat capacity data.
7. Description of any recently obtained heat capacity results, including error plot, on a Reference Material traceable to a national standards organization, or results on a material with well-known heat capacity values (include text file of accepted values and literature reference), that were used to determine the accuracy of the instrument and test procedure used. Materials used for this check should be different from that used as the standard reference material for the current measurements. (Example: Do not test a sapphire specimen as an accuracy test if sapphire is your reference material.)
8. Description of temperature scale calibration including method, materials used, frequency, last calibration date, etc.
9. In addition to heat capacity results, please transmit any raw instrument files used to calculate heat capacity in a text file format including file information such as specimen weight, ramp rates, purge gas and flow rate, date, etc. Data output should include time, temperature, and heat flow. Data files transmitted should include baseline, reference and specimen under test for each specimen tested.

3. Test procedure for Seebeck coefficient and electrical resistivity:

The standard Seebeck coefficient and electrical resistivity tests are performed on a single specimen. The test procedures for simultaneous measurements are described below:

Specimen: The standard Seebeck coefficient and electrical resistivity tests are performed on a single specimen. The ideal specimen is a long cylinder or bar. For typical thermoelectrics, geometries such as a 2 mm x 2 mm x 15 mm bar or a 3 mm x 3 mm x 12 mm bar are sufficient. The specimens need to be machined with parallel surfaces. The top and bottom surfaces need to be flat and parallel to ensure good contacts. Specimen dimensions need to be determined using a calibrated micrometer. The voltage probe spacing needs to be determined for each measurement. A better solution is to use a digital microscope and the measured sample width as calibration from the same image. The center-to-center distance of the voltage probes is used.

Seebeck coefficient and resistivity tests: The Seebeck coefficient and resistivity is usually performed using the potentiometric (4-probe) or the axial flow (2-probe) method. For high temperature measurements, the test environment is usually vacuum, or very low pressure static helium or flowing argon. Seebeck coefficient can be measured by slowly ramping the furnace or the differential method in which the sample is stabilized at a set point and a small ΔT is applied across the specimen. To determined Seebeck coefficient several ΔT is used and the slope of the ΔV vs. ΔT curve gives the total Seebeck coefficient of the circuit. To obtain the true Seebeck value of the specimen the Seebeck value of the probe material needs to be subtracted. The values for the probe are available for the thermocouple used (k or R-type thermocouple) and provided as a look-up table.

In the differential method, it is preferred to measure electrical resistivity before the ΔT is established at each set point for Seebeck measurements. Due to the Joule heating and Peltier effect of thermoelectric, the temperature gradient may be generated and cause measurement error. In order to eliminate this effect, the current is usually reversed quickly without altering the voltage measurement polarity. However, in order to minimize the Peltier effect the measurements must be completed within one second or even faster.

There are other techniques to measure electrical resistivity such as 4-point probe (in-line probes) or the Van Der Pauw technique. For the in-line probe method, it is important to recognize the measurement is more accurate for isotropic thin specimens. Measurements on materials with layered structures, such as Bi_2Te_3 must be analyzed carefully since resistivity depends on orientation and how the specimen is cut. The Van Der Pauw is suitable for very thin specimens (<0.5 mm) and it is also a surface resistivity measurement.

Calibration: The Seebeck values are less dependent on sample geometry. However, it is a common practice to place the probes away from the current contact to avoid non-uniform heat areas. The system should be calibrated using a reference material with known Seebeck values (such as Constantan for certain commercial system). The Seebeck values of the measured references need to be within the specified accuracy limits. If it is drifting outside the acceptable range, a new probe is needed.